



## Original Article

# Electrochemical Sensor Based on Ce-MOF Modified Screen Printed Electrode for Metronidazole Determination

Peyman Mohammadzadeh Jahani<sup>1</sup>, Somayeh Tajik<sup>2,\*</sup>, Zahra Dourandish<sup>2</sup><sup>1</sup>School of Medicine, Bam University of Medical Sciences, Bam, Iran<sup>2</sup>Research Center for Tropical and Infectious Diseases, Kerman University of Medical Sciences, Kerman, Iran

## ARTICLE INFO

## Article history

Submitted: 2023-11-17

Revised: 2024-01-19

Accepted: 2024-01-26

Manuscript ID: CHEMM-2312-1750

Checked for Plagiarism: Yes

Language Checked: Yes

DOI:10.48309/CHEMM.2024.431008.1750

## KEYWORDS

Ce-BTC metal-organic framework  
Screen-printed graphite electrode  
Electrochemical sensor  
Metronidazole

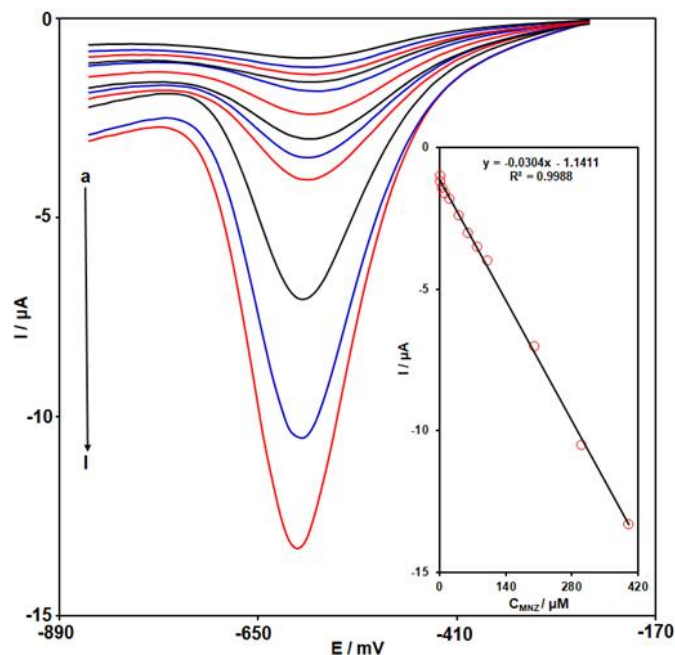
## ABSTRACT

In the present study, a fast, sensitive, and simple electrochemical sensor based on screen-printed graphite electrode (SPGE) modified with Ce-1,3,5-benzenetricarboxylic acid (Ce-BTC) metal-organic framework (MOF) has been prepared for determination of metronidazole (MNZ). The electrochemical studies and measurements were done using cyclic voltammetry (CV), linear sweep voltammetry (LSV), differential pulse voltammetry (DPV), and chronoamperometry techniques. Comparison study of electrochemical performance of unmodified SPGE and Ce-BTC MOF/SPGE toward the reduction of MNZ was evaluated by using CV. The CV studies show that modification of SPGE surface with Ce-BTC MOF enhances the reduction peak current but the peak potential of MNZ has shifted to the lower potential. Using the effects of Ce-BTC MOF, the developed modified SPGE showed good electrochemical sensing performance for detecting MNZ in phosphate buffer solution (PBS) (pH = 7.0) with wide linear range (0.05-400.0  $\mu\text{M}$ ), high sensitivity (-0.0304  $\mu\text{A}/\mu\text{M}$ ), and low limit of detection (LOD) (0.02  $\mu\text{M}$ ). Finally, for the MNZ analysis in real samples, the Ce-BTC MOF/SPGE sensor exhibited good MNZ determination performance with acceptable recoveries of 96.7%-103.6% and low relative standard deviation (RSD) values of 1.8%-3.5%.

\* Corresponding author: Somayeh Tajik

E-mail: [tajik\\_s1365@yahoo.com](mailto:tajik_s1365@yahoo.com)

© 2024 by SPC (Sami Publishing Company)



## Introduction

Metronidazole (MNZ) is a member of the nitroimidazole antibiotic family and its frequently employed to treat infections induced by protozoa and anaerobic bacteria in humans and domestic animals [1]. Despite its effective antibacterial properties, the long-term abuse of MNZ poses a significant risk in the health of both humans and animals owing to its genotoxic, carcinogenic, and mutagenic side effects [2]. Consequently, it is crucial to find a sensitive, fast, and efficient method to detect and measure the MNZ level in various compounds and biological fluids. So far, several techniques have been used for the MNZ determination in pharmaceutical compounds, biological fluids, and environmental samples [3,4]. The electrochemical methods have attracted broad attention to determine multiple and various compounds owing to their relatively simple and low-cost equipment, easy and simple operation, fast response, portability, and minimal sample preparation [5-9]. Screen-printing has been suggested in the microelectronics field as a technology for mass production of reliable, inexpensive, reproducible, and disposable sensors, serving as an on-site monitoring approach. In recent years, electrochemical sensors based on SPEs have appeared as one of the main fields of electrochemical research for

sensitive, fast, specific, low cost and portable analyses, and have potential innovative applications [10,11].

The ability for trace amounts of compounds with high sensitivity of electrochemical sensors is crucial to expand the practical application of electrochemical analysis. Therefore, in the fabrication and design of electrochemical sensing platforms, using and selecting the appropriate materials as the modifying agents is the primary challenge [12-14]. In contrast to bulk materials, nanostructured materials demonstrate enhanced performance in various applications due to their distinctive structural features [15-27]. Particularly, according to the recent studies, the use of nanomaterials in fabrication of electrochemical sensors has been confirmed to further improve their detection performance [28-31].

MOFs or coordination polymers are a new class of nano-porous materials, which are comprised of metal ions and organic ligands. The self-assembly of metal ions with organic ligands in the form of a crystal structure has provided a suitable opportunity to create diverse and abundant compounds with high flexibility in the structure, shape, and the size of pores. The wide diversity of MOFs has provided a high capability of wide applications in different fields including drug delivery, catalysis, separation, water

purification, and etc. [32]. Especially, recent research in this field has shown that nanostructured MOFs are among the most widely used compounds in the field of sensor technology [33,34]. The prominent features of these compounds compared to other porous materials are high porosity, high surface area, adjustable pore size, and uniform structure of the pores. Here, the Cu-BTC MOF was synthesized and used to fabricate an electrochemical sensor for MNZ determination. Compared to the unmodified SPGE, at the Cu-BTC MOF/SPGE an enhancement in the reduction peak current at reduced overpotential for MNZ was observed. The as-fabricated Cu-BTC MOF/SPGE sensor also provided a high sensitivity ( $-0.0304 \mu\text{A}/\mu\text{M}$ ) toward MNZ reduction with a linear range of  $0.05\text{-}400.0 \mu\text{M}$ . Finally, the evaluation of modified SPGE performance for detection of MNZ in MNZ tablets and urine samples was investigated.

## Experimental

### Reagents and Instruments

All reagents used during the experiments were of analytical grade. They were provided from Sigma-Aldrich and Merck companies and employed without any processing.

Electrochemical studies and measurements were done using SPGE (DropSens (Spain)-DRP-110) consisting of working electrode (graphite), graphite-based counter electrode, and silver (Ag) pseudo-reference electrode. The SPGE was connected to an Autolab PGSTAT 302 N electrochemical workstation (Metrohm, Switzerland). Likewise, the Autolab was connected to a computer for data storage and processing.

The synthesis and characterization of Ce-BTC MOF was reported in our previous work [35]. The FE-SEM image of prepared MOF (Ce-BTC MOF) is displayed in Figure 1.

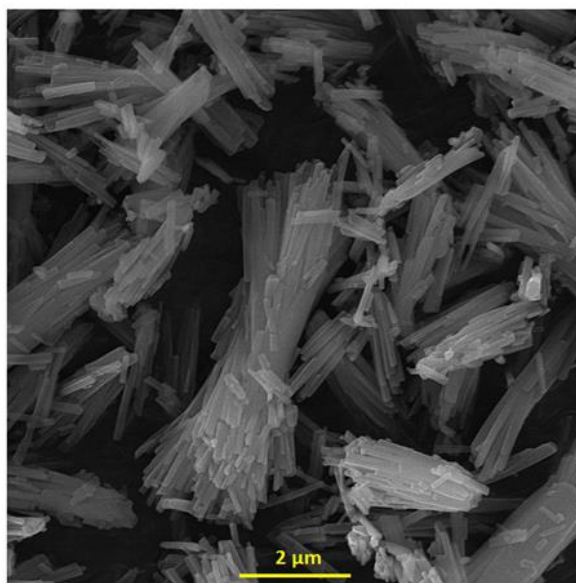


**Figure 1:** The FE-SEM image of Ce-BTC MOF

### SPGE Modification

To modify the SPGE surface, the prepared Ce-BTC MOF was dispersed into deionized water ( $1 \text{ mg/mL}$ ), and ultrasonicated for at least 20 min to ensure the full dispersion, and then  $3 \mu\text{L}$  of this suspension was drop-casted on the surface of SPGE. After that, the prepared SPGE was dried at

ambient temperature to obtain Ce-BTC MOF/SPGE.

To calculate the surface area of the unmodified SPGE and Ce-BTC MOF modified SPGE, the CVs were recorded at various scan rates in  $0.1 \text{ M KCl}$  solution containing  $1.0 \text{ mM K}_3[\text{Fe}(\text{CN})_6]$  (Redox probe). Using the Randles-Sevcik equation, the value of surface area of Ce-BTC MOF/SPGE was

calculated to be 0.116 cm<sup>2</sup>, which was 3.7 times greater than the surface area of unmodified SPGE.

## Results and Discussion

### Comparison of Electrochemical Behavior of MNZ on Unmodified SPGE and Ce-BTC MOF Modified SPGE

The response of Ce-BTC MOF/SPGE toward MNZ (35.0 μM) in 0.1 M PBS (pH = 7.0) in a range of pH values from 2.0 to 9.0 was evaluated by using DPV. The pH of PBS (supporting electrolyte) showed a significant effect on the reduction peak

of MNZ. According to the resulting voltammograms, the maximum intensity of the cathodic peak current (*I*<sub>pc</sub>) was detected at pH = 7.0. Therefore, other electrochemical studies and measurements were done in 0.1 M PBS (pH = 7.0).

Figure 2 presents the comparison of unmodified SPGE (a) and Ce-BTC MOF/SPGE (b) toward MNZ determination in 0.1 M PBS (pH = 7.0) by using CV. As can be seen, on the unmodified SPGE a weak response was observed for the reduction reaction of MNZ. Compared with unmodified SPGE, the Ce-BTC MOF modified SPGE showed a cyclic voltammogram with an increased *I*<sub>pc</sub> (10.5 μA) and decreased over-potential (-605 mV).

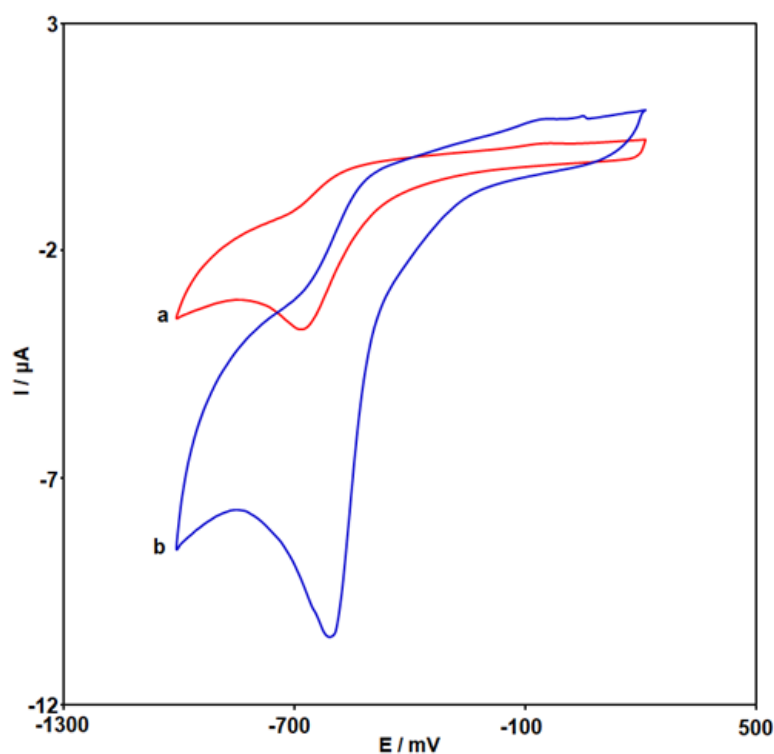


**Figure 2:** CVs obtained from 300.0 μM MNZ solution in 0.1 M PBS (pH = 7.0) at unmodified SPGE (a) and Ce-BTC MOF/SPGE (b) (scan rate of 50 mV/s)

### Evaluation of the Influence of Scan Rate on the Electrochemical Reduction of MNZ

The voltammetric behavior of MNZ was studied in a range of scan rates (from 5 to 100 mV/s) at Ce-BTC MOF/SPGE by using LSV (Figure 3). For each scan rate, a well-defined reduction peak was

detected and the *I*<sub>pc</sub> continuously improved with an increase in scan rate. The observed linear relationship between *I*<sub>pc</sub> and the square root of the scan rate ( $v^{1/2}$ ) demonstrates that the reduction process is mainly diffusion controlled (Figure 3-Inset) with a linear equation expressed as  $I_{pc} (\mu A) = -1.0387v^{1/2} + 0.3751$  ( $R^2 = 0.9993$ ).

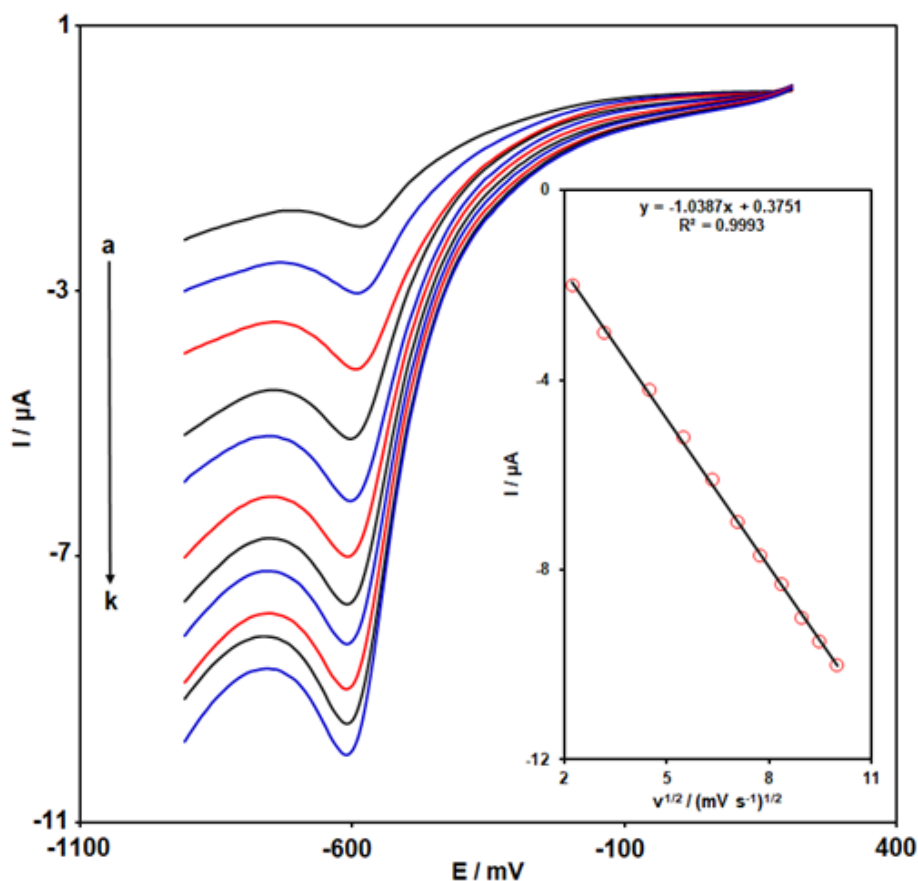


**Figure 3:** LSVs obtained from MNZ solution (200.0  $\mu\text{M}$ ) in 0.1 M PBS (pH = 7.0) at scan rates of (a) 5, (b) 10), (c) 20, (d) 30, (e) 40, (f) 50, (g) 60, (h) 70, (i) 80, (j) 90, and (k) 100 mV/s. Inset: Plot of  $I_{pc}$  vs.  $v^{1/2}$

### Chronoamperometric Measurements

The electrochemical reduction of MNZ at Ce-BTC MOF/SPGE was also studied by using chronoamperometry. For this purpose, the chronoamperometric measurements of MNZ were performed in 0.1 M PBS (pH = 7.0) containing variable concentrations of MNZ by applying an appropriate potential step of -650 mV. The recorded chronoamperograms (plots of current intensity ( $\mu\text{A}$ ) vs. time (s)) for different concentrations of MNZ (0.1 mM to 1.5 mM) is demonstrated in Figure 4. The resulting chronoamperograms show the dependence of current intensity on time. From chronoamperometric measurements, the diffusion coefficient ( $D$ ) can be calculated using the Cottrell's equation ( $I = nFAD^{1/2}C/\pi^{1/2}t^{1/2}$ ). The plot of current intensity ( $\mu\text{A}$ ) vs.  $t^{-1/2}$  showed a good linear dependence between these two variables for each concentration (Figure 4A), and then by drawing the plot of the resulting slopes

from Figure 4A vs. MNZ concentrations (Figure 4B), the value of  $D$  ( $1.5 \times 10^{-6} \text{ cm}^2/\text{s}$ ) was calculated.

### Electrochemical Quantification of MNZ Using DPV

The DPV responses of Ce-BTC MOF/SPGE in 0.1 M PBS containing variable concentrations of MNZ were revealed in Figure 5 in the following conditions: step potential 0.01 V and pulse amplitude 0.025 V. As can be seen, the peak currents of DPV enhances along with increasing MNZ concentration, showing the strong response of Ce-BTC MOF/SPGE to MNZ. Furthermore, Figure 5-Inset displays the corresponding the calibration plot related to the obtained responses. The MNZ concentration and the related  $I_{pc}$  value demonstrated a clear linear relationship from 0.05  $\mu\text{M}$  to 400.0  $\mu\text{M}$ . The LOD value was calculated 0.02  $\mu\text{M}$ . The performance of the Ce-BTC MOF/SPGE sensor with some of reported works in the literature for MNZ determination is presented in Table 1.

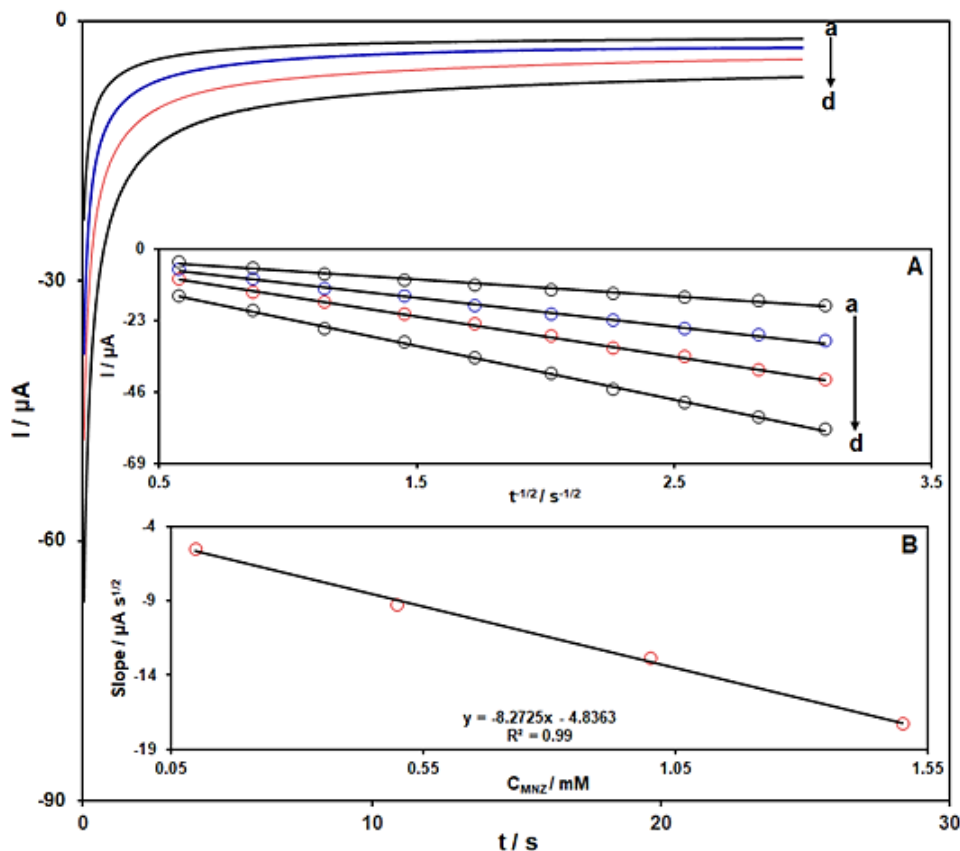


**Figure 4:** Chronoamperometric response of Ce-BTC MOF/SPGE in 0.1 M PBS (pH = 7.0) for a (0.1), b (0.5), c (1.0), and d (1.5) mM of MNZ. Inset A (Plots of  $I_{pc}$  vs.  $t^{1/2}$  for recorded chronoamperograms) and Inset B (Plot of the slope of the obtained lines vs. MNZ concentration)

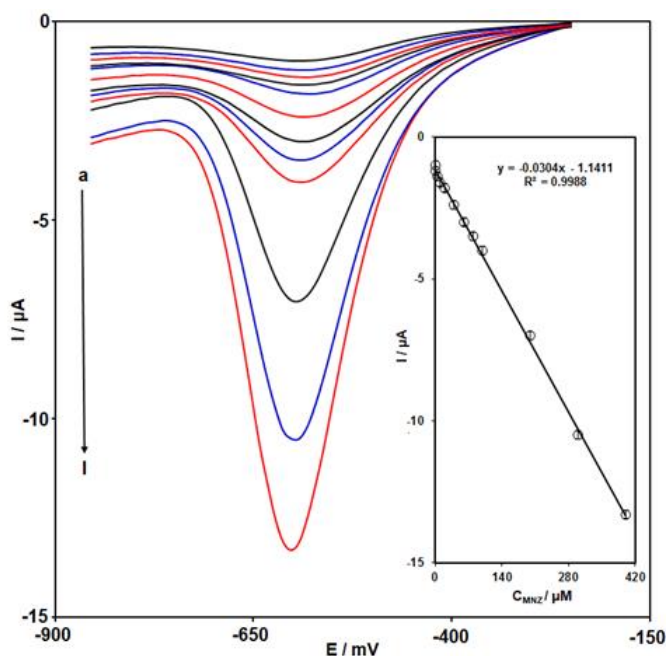


**Figure 5:** DPV responses of Cu-BTC MOF/SPGE in 0.1 M PBS containing MNZ a (0.05), b (1.0), c (5.0), d (10.0), e (20.0), f (40.0), g (60.0), h (80.0), i (100.0), j (200.0), k (300.0), and l (400.0)  $\mu\text{M}$ . Inset: The plot of  $I_{pc}$  against the MNZ concentration

**Table 1:** Comparison of the Ce-BTC MOF/SPGE sensor with previously reported MNZ sensors

Electrochemical Sensor	Electrochemical Method	Linear Range	LOD	Ref.
Graphene-bismuth/glassy carbon electrode (GCE)	CV	0.005 - 260 $\mu\text{M}$	0.9 nM	[1]
$\beta$ -cyclodextrin-functionalized gold nanoparticles/poly(L-cysteine)/GCE	Linear sweep stripping voltammetry (LSSV)	0.1 - 600 $\mu\text{M}$	14 nM	[2]
Ag/Au Modified Nafion Coated GCE	DPV	$1.00 \times 10^{-4}$ - $1.00 \times 10^{-3}$ M	$5.87 \times 10^{-8}$ M	[3]
Flower-like cobalt anchored on reduced graphene oxide (f-Co@rGO) nanocomposite/GCE	DPV	0.025 - 500 nM	0.015 nM	[4]
Ce-BTC MOF/SPGE	DPV	0.05 - 400.0 $\mu\text{M}$	0.02 $\mu\text{M}$	This work

### MNZ Detection in Urine and Tablet Samples

To investigate the applicability of Ce-BTC MOF/SPGE as electrochemical sensor for determination of MNZ in urine and MNZ tablet samples, the analytical tests using the standard addition method by DPV were done in 0.1 M PBS containing prepared real samples. The results of

DPV measurements for MNZ determination were presented in Table 2.

The obtained suitable values of recovery (96.7%-103.6%) and acceptable values of RSD (1.8%-3.5%) confirm the accuracy, precision, and as well as applicability of the prepared sensor for determination of MNZ contents in real samples.

**Table 2:** The results obtained for determination of MNZ contents in prepared urine and MNZ tablets using DPV measurements on the Ce-BTC MOF/SPGE (n = 5)

Sample	Spiked concentration ( $\mu\text{M}$ )	Found concentration ( $\mu\text{M}$ )	Recovery (%)	R.S.D. (%)
MNZ tablet	0	5.3	-	3.4
	1.0	6.2	98.4	2.3
	2.0	7.5	102.7	2.9
	3.0	8.6	103.6	1.8
	4.0	9.2	98.9	2.2
Urine	0	-	-	-
	4.0	4.1	102.5	1.9
	6.0	5.8	96.7	3.5
	8.0	8.1	101.2	2.1
	10.0	9.9	99.0	2.7

### Conclusion

To sum up, an electrochemical sensor based on Ce-BTC MOF modified SPGE was used to detect MNZ. The electrochemical studies by using CV showed that the Ce-BTC MOF modified SPGE effectively improved the electrochemical reduction of MNZ compared to unmodified SPGE. After optimizing the parameters, the modified SPGE sensor was applied to determine MNZ by using DPV. Concerning optimum conditions, the

Ce-BTC MOF modified SPGE showed a linear response to MNZ between 0.05  $\mu\text{M}$  and 400.0  $\mu\text{M}$  with LOD of 0.02  $\mu\text{M}$  using DPV. Finally, the standard addition method was demonstrated good ability of Ce-BTC MOF/SPGE to determine of MNZ in real samples.

### Disclosure Statement

No potential conflict of interest was reported by the authors.

## Funding

This study did not receive any specific grant from funding agencies in the public, commercial, or not-for-profit sectors.

## Authors' Contributions

All authors contributed toward data analysis, drafting, and revising the paper and agreed to responsible for all the aspects of this work.

## Conflict of Interest

The authors declare that they have no conflicts of interest in this article.

## References

- [1]. Yu T., Glennon L., Fenelon O., Breslin C.B., Electrodeposition of bismuth at a graphene modified carbon electrode and its application as an easily regenerated sensor for the electrochemical determination of the antimicrobial drug metronidazole, *Talanta*, 2023, **251**:123758 [Crossref], [Google Scholar], [Publisher]
- [2]. Gu Y., Liu W., Chen R., Zhang L., Zhang Z.,  $\beta$  - Cyclodextrin - functionalized gold nanoparticles/Poly (L-cysteine) modified glassy carbon electrode for sensitive determination of metronidazole, *Electroanalysis*, 2013, **25**:1209 [Crossref], [Google Scholar], [Publisher]
- [3]. Khanfar M.F., Al Absi N., Abu-Nameh E.S., Saket M.M., Khorma N., Al Daoud R., Alnuman N., Ag/Au modified nafion coated glassy carbon electrode for the detection of metronidazole, *International Journal of Electrochemical Science*, 2019, **14**:3265 [Crossref], [Google Scholar], [Publisher]
- [4]. Huang J., Qiu Z., Lin J., Lin J., Zhu F., Lai G., Li Y., Ultrasensitive determination of metronidazole using flower-like cobalt anchored on reduced graphene oxide nanocomposite electrochemical sensor, *Microchemical Journal*, 2023, **188**:108444 [Crossref], [Google Scholar], [Publisher]
- [5]. Garkani Nejad F., Tajik S., Beitollahi H., Sheikhshoaei I., Magnetic nanomaterials based electrochemical (bio) sensors for food analysis,

*Talanta*, 2021, **228**:122075 [Crossref], [Google Scholar], [Publisher]

- [6]. Resen N.D., Gomaa E.A., Salem S.E., Abd El-Hady M.N., El-Defrawy A.M., Voltammetric analysis of lead nitrate with various ligands in aqueous solutions at 302.15 K, *Chemical Methodologies*, 2023, **7**:761 [Crossref], [Google Scholar], [Publisher]

- [7]. Mustafa Y.F., Chehardoli G., Habibzadeh S., Arzehgar, Z., Electrochemical detection of sulfite in food samples. *Journal of Electrochemical Science and Engineering*, 2022, **12**:1061 [Google Scholar], [Publisher]

- [8]. Cerda V., Rennan G.O.A., Ferreira S.L., Revising flow-through cells for amperometric and voltammetric detections using stationary mercury and bismuth screen printed electrodes, *Progress in Chemical and Biochemical Research*, 2022, **5**:351 [Crossref], [Google Scholar], [Publisher]

- [9]. Mhaibes R. M., Arzehgar Z., Mirzaei Heydari M., Fatolahi L. ZnO Nanoparticles: A Highly Efficient and Recyclable Catalyst for Tandem Knoevenagel-Michael-Cyclocondensation Reaction, *Asian Journal of Green Chemistry*, 2023, **7**:1 [Crossref], [Google Scholar], [Publisher]

- [10]. Tajik S., Beitollahi H., Jang H.W., Shokouhimehr M., A screen printed electrode modified with Fe<sub>3</sub>O<sub>4</sub>@polypyrrole-Pt core-shell nanoparticles for electrochemical detection of 6-mercaptopurine and 6-thioguanine, *Talanta*, 2021, **232**:122379 [Crossref], [Google Scholar], [Publisher]

- [11]. Liu M.M., Zhang F.F., Liu H., Wu M.J., Liu Z.J., Huang P.F., Cell viability and drug evaluation biosensing system based on disposable AuNPs/MWCNT nanocomposite modified screen-printed electrode for exocytosis dopamine detection, *Talanta*, 2023, **254**:124118 [Crossref], [Google Scholar], [Publisher]

- [12]. Mehdizadeh Z., Shahidi S., Ghorbani-HasanSarai A., Limooei M., Bijad M., Monitoring of amaranth in drinking samples using voltammetric amplified electroanalytical sensor, *Chemical Methodologies*, 2022, **6**:246 [Crossref], [Google Scholar], [Publisher]

- [13]. Pyman H., Design and fabrication of modified DNA-Gp nano-biocomposite electrode for industrial dye measurement and optical confirmation, *Progress in Chemical and Biochemical Research*, 2022, **5**:391 [[Crossref](#)], [[Google Scholar](#)], [[Publisher](#)]
- [14]. Roshanfekar H., A simple specific dopamine aptasensor based on partially reduced graphene oxide–AuNPs composite, *Progress in Chemical and Biochemical Research*, 2023, **6**:61 [[Crossref](#)], [[Google Scholar](#)], [[Publisher](#)]
- [15]. Akeremale O.K., Metal-organic frameworks (MOFs) as adsorbents for purification of dye-contaminated wastewater: a review, *Journal of Chemical Reviews*, 2022, **4**:1 [[Crossref](#)], [[Google Scholar](#)], [[Publisher](#)]
- [16]. Baghernejad B., Alikhani M., Nano-cerium oxide/aluminum oxide as an efficient catalyst for the synthesis of xanthene derivatives as potential antiviral and anti-inflammatory agents, *Journal of Applied Organometallic Chemistry*, 2022, **2**:140 [[Crossref](#)], [[Google Scholar](#)], [[Publisher](#)]
- [17]. Alao I., Oyekunle I., Iwuzor K., Emenike E., Green synthesis of copper nanoparticles and investigation of its antimicrobial properties, *Advanced Journal of Chemistry, Section B*, 2022, **4**:39 [[Crossref](#)], [[Google Scholar](#)], [[Publisher](#)]
- [18]. Palke D., Synthesis, physicochemical and biological studies of transition metal complexes of DHA schiff bases of aromatic amine, *Journal of Applied Organometallic Chemistry*, 2022, **2**:81 [[Crossref](#)], [[Google Scholar](#)], [[Publisher](#)]
- [19]. Daliri Shamsabadi O., Investigation of antimicrobial effect and mechanical properties of modified starch films, cellulose nanofibers, and citrus essential oils by disk diffusion method, *Asian Journal of Green Chemistry*, 2024, **8**:1 [[Crossref](#)], [[Google Scholar](#)], [[Publisher](#)]
- [20]. Alinezhad H., Hajiabbas Tabar Amiri P., Mohseni Tavakkoli S., Muslim Muhiebes R., Fakri Mustafa Y., Progressive types of Fe<sub>3</sub>O<sub>4</sub> nanoparticles and their hybrids as catalysts, *Journal of Chemical Reviews*, 2022, **4**:288 [[Crossref](#)], [[Google Scholar](#)], [[Publisher](#)]
- [21]. Arzehgar Z., Aydi A., Mirzaei Heydari M. Silver functionalized on hydroxyapatite-core-shell magnetic  $\gamma$ -Fe<sub>2</sub>O<sub>3</sub>: An environmentally and readily recyclable nanocatalyst for the one-pot synthesis of 14H-dibenzo[a,j]xanthenes derivatives, *Asian Journal of Green Chemistry*, 2018, **2**:281 [[Crossref](#)], [[Google Scholar](#)], [[Publisher](#)]
- [22]. Janitabar Darzi S., Bastami H., Au decorated mesoporous TiO<sub>2</sub> as a high performance photocatalyst towards crystal violet dye, *Advanced Journal of Chemistry, Section A*, 2022, **5**:22 [[Crossref](#)], [[Google Scholar](#)], [[Publisher](#)]
- [23]. Hakimi F., Golrasan E., Zinc sulfide (ZnS) nanoparticles: an effective catalyst for synthesis of benzoxazole derivatives, *Asian Journal of Green Chemistry*, 2023, **7**:47 [[Crossref](#)], [[Google Scholar](#)], [[Publisher](#)]
- [24]. Kadhim Q., Alfalluji A., Essa F., Characterization of nanofibrous scaffolds for nanomedical applications involving poly (methyl methacrylate)/poly (vinyl alcohol), *Journal of Medicinal and Pharmaceutical Chemistry Research*, 2023, **5**:720 [[Publisher](#)]
- [25]. Awan M.N., Razzaq H., Abid O.U., Qaisar S., Recent advances in electroanalysis of hydrazine by conducting polymers nanocomposites: a review, *Journal of Chemical Reviews*, 2023, **5**:311 [[Crossref](#)], [[Google Scholar](#)], [[Publisher](#)]
- [26]. Patil V., Singh R., Kanade K., Yi G.R., Copper nanomaterials derived preventive technologies for COVID-19 pandemic: a review, *Advanced Journal of Chemistry, Section A*, 2022, **5**:1 [[Crossref](#)], [[Google Scholar](#)], [[Publisher](#)]
- [27]. Heidariipour A., Salmani F., Barati T., Synthesis of coral-like ZnO nanostructures with high and wide absorption range, *Asian Journal of Green Chemistry*, 2023, **7**:140 [[Crossref](#)], [[Google Scholar](#)], [[Publisher](#)]
- [28]. Sengar M., Saxena S., Satsangee S., Jain R., Silver nanoparticles decorated functionalized multiwalled carbon nanotubes modified screen printed sensor for the voltammetric determination of butorphanol, *Journal of Applied Organometallic Chemistry*, 2021, **1**:95 [[Crossref](#)], [[Google Scholar](#)], [[Publisher](#)]
- [29]. Beitollahi H., Arbabi N., Nanolayered Ti<sub>3</sub>C<sub>2</sub> modified screen printed electrode as high-performance electrode for electrochemical detection of tyrosine, *Chemical Methodologies*,

- 2022, **6**:293 [[Crossref](#)], [[Google Scholar](#)], [[Publisher](#)]
- [30]. Tajik S., Beitollahi H., Garkani Nejad F., Safaei M., Zhang K., Van Le Q., Varma R.S., Jang H.W., Shokouhimehr M., Developments and applications of nanomaterial-based carbon paste electrodes, *RSC Advances*, 2020, **10**:21561 [[Crossref](#)], [[Google Scholar](#)], [[Publisher](#)]
- [31]. Mohammadi S.Z., Beitollahi H., Bani Asadi E., Electrochemical determination of hydrazine using a ZrO<sub>2</sub> nanoparticles-modified carbon paste electrode, *Environmental Monitoring and Assessment*, 2015, **187**:1 [[Crossref](#)], [[Google Scholar](#)], [[Publisher](#)]
- [32]. He T., Kong X.J., Li J.R., Chemically stable metal-organic frameworks: rational construction and application expansion, *Accounts of Chemical Research*, 2021, **54**:3083 [[Crossref](#)], [[Google Scholar](#)], [[Publisher](#)]
- [33]. Dourandish Z., Tajik S., Beitollahi H., Mohammadzadeh Jahani P., Garkani Nejad F., Sheikhshoae I., Di Bartolomeo A., A Comprehensive review of metal-organic framework: synthesis, characterization, and investigation of their application in electrochemical biosensors for biomedical analysis, *Sensors*, 2022, **22**:2238 [[Crossref](#)], [[Google Scholar](#)], [[Publisher](#)]
- [34]. Han S., Sun R., Zhao L., Yan C., Chu H., Molecularly imprinted electrochemical sensor based on synergistic interaction of honeycomb-like Ni-MOF decorated with AgNPs and N-GQDs for ultra-sensitive detection of olaquinox in animal-origin food, *Food Chemistry*, 2023, **418**:136001 [[Crossref](#)], [[Google Scholar](#)], [[Publisher](#)]
- [35]. Tajik S., Sharifi F., Aflatoonian B., Di Bartolomeo A., A new electrochemical sensor for the detection of ketoconazole using carbon paste electrode modified with sheaf-like Ce-BTC MOF nanostructure and ionic liquid, *Nanomaterials*, 2023, **13**:523 [[Crossref](#)], [[Google Scholar](#)], [[Publisher](#)]

#### HOW TO CITE THIS ARTICLE

Peyman Mohammadzadeh Jahani, Somayeh Tajik, Zahra Dourandish. Electrochemical Sensor Based on Ce-MOF Modified Screen Printed Electrode for Metronidazole Determination. *Chem. Methodol.*, 2024, 8(2) 123-132

DOI: <https://doi.org/10.48309/CHEMM.2024.431008.1750>

URL: [https://www.chemmethod.com/article\\_189580.html](https://www.chemmethod.com/article_189580.html)